Helium Atom Scattering from C_2H_6, F_2HCCH_3, F_3CCH_2F and C_2F_6 in Crossed Molecular Beams

Markus Hammer and Wolfhart Seidel

Physikalisch-Chemisches Institut, Justus-Liebig-Universität Gießen, Heinrich-Buff-Ring 58, D-35392 Gießen

Z. Naturforsch. **52 a,** 695–701 (1997); received August 8, 1997

Rotationally unresolved differential cross sections were measured in crossed molecular beam experiments by scattering Helium atoms from Ethane, 1,1-Difluoroethane, 1,1,1,2-Tetrafluoroethane and Hexafluoroethane. The damping of observed diffraction oscillations was used to extract anisotropic interaction potentials for these scattering systems applying the infinite order sudden approximation (IOSA). Binary macroscopic parameters such as second heterogeneous virial coefficients and the coefficients of diffusion and viscosity were computed from these potentials and compared to results from macroscopic experiments.

Key words: Molecular beams, Helium, Interaction potential, Fluoroethanes, Binary coefficients.

I. Introduction

As has been reported previously [1 - 5] reliable potentials for the interaction between He atoms and even rather anisotropic molecules can be determined from rotationally unresolved total differential cross sections (DCS), observed in respective scattering experiments using crossed molecular beams. Results of an infinite order sudden approximation (IOSA) [6 - 9] were fitted to the observed DCS using a modified Hartree Fock dispersion potential (HFD) [10] to model the scattering interaction. Since macroscopic coefficients such as the binary second virial coefficient, the diffusivity and the coefficient of viscosity are theoretically related to the interaction potential, these parameters can be determined by first-order computations and compared to results from macroscopic experiments if available [3].

II. Experiment

The crossed-beam apparatus has already been described in detail in [1, 4]. Its main features are two supersonic nozzle sources for the He atom beam and the molecular beam, intersecting rectangularly. A quadrupole mass spectrometer detector which can be rotated in-plane with respect to both beams is used to detect the angle dependent scattering intensity of He atoms. This detector was also used for beam profile optimization and for time-of-flight analysis of either beam. From the pressure dependence of the speed ratio S for the beams of the ethanes, cluster formation, which would disturbe the DCS observations [4], could be inferred to be negligable in the region of the respective source pressure. Scattering curves were measured by rotating the detector automatically in steps of 0.2° from 22° down to 3°. In order to reduce the signal to noise ratio, these curves were measured repeatedly up to 12 times. Experimental conditions and operational parameters are summarized in Table 1.

Table 1. Beam conditions.

	He	C_2H_6	1,1-$C_2H_4F_2$	1,1,1,2-$C_2H_2F_4$	C_2F_6
Substance purity (%)	99.998	99.95	> 98	98.5	> 98
Source pressure (bar)	45	0.20	0.30	0.20	0.30
Nozzle diameter (μm)	20	100	100	100	100
Temperature (K)	298	305	355	355	355
Skimmer diameter (mm)	0.3	0.5	0.5	0.5	0.5
Nozzle-skimmer distance (mm)	20	2.0	2.0	2.0	2.0
Collimator diameter (mm)	1.0	—	—	—	—
Most probable velocity (ms^{-1})	1625	860	652	538	460
Collision energy (meV)		61.8	59.9	58.4	57.4
Angular divergence (degree)	0.9	9.3	7.9	6.8	7.3
Speed ratio S	40	3.5	3.8	5.3	4.8

Reprint requests to Prof. Dr. W. Seidel,
Fax: +49 641 99 34509.

0932-0784 / 97 / 1000-0695 $ 06.00 © – Verlag der Zeitschrift für Naturforschung, D-72072 Tübingen

III. Analysis and fitting

A) Interaction potential

As in previous investigations [1 - 5*] a modified Hartree Fock dispersion potential (HFD) (as presented by Aziz et al. [10]) was used for the central part. The constants of the potential equations, i. e. a and c_n, were defined in their reduced form.

$$V(R) = \varepsilon_m f(r), \tag{1}$$

$$r = \frac{R}{R_m}, \tag{2}$$

$$f(r) = f_{rep}(r) + f_{att}(r)d(r), \tag{3}$$

$$f_{rep}(r) = a \exp[-b(r-1)], \tag{4}$$

$$f_{att}(r) = -\left(\frac{c_6}{r^6} + \frac{c_8}{r^8} + \frac{c_{10}}{r^{10}}\right), \tag{5}$$

$$d(r) = \begin{cases} e^{-\left(\frac{1.28}{r}-1\right)^2} & \text{for} \quad r \leq 1.28 \\ 1 & \text{for} \quad r > 1.28 \end{cases}, \tag{6}$$

$$c_n = \frac{C_n}{R_m^n \varepsilon_m}, \tag{7}$$

$$a = \frac{A}{\varepsilon_m}. \tag{8}$$

According to Douketis [11], $c_{10} \approx 1.225(c_8^2/c_6)$; and the constants a and b of (4) can be calculated from the minimum conditions of the respective potential. Anisotropy was introduced to the potential by expanding the energy parameter, ε_m, and the range parameter, R_m, as follows [12]

$$\varepsilon_m = \varepsilon_0 + C_1\varepsilon_1 + C_2\varepsilon_3 + C_3\varepsilon_4, \tag{9}$$

$$R_m = R_0 + C_1R_1 + C_2R_3 + C_3R_4, \tag{10}$$

with

$$C_1 = 1 - R_2 \sin\theta, \tag{11}$$

$$C_2 = \cos\theta, \tag{12}$$

$$C_2 = \cos^2\theta, \tag{13}$$

where θ is the (orientational) polar angle. Although only a small number of adjustable parameters is needed, the main advantage of this rotationally symmetric potential model (CIG) is its flexibility. It may properly be used to portray a ball as well as a dumpbell or a *cigar* shaped object.

C) Data Analysis and Fitting

To analyze the observed DCS results, the IOSA procedure [6 - 9] was used. This is justified because, as shown by Frick [13], the rotational levels of the molecules, even for rather large values of j, are very close together. Therefore, since the collision energy is about 60 meV, the energy sudden part of the IOSA should be valid. Also its centrifugal sudden part is suitable, since anisotropic interaction is confined to a rather limited space around the molecular center. Using phase shifts from the semiclassical JWKB approximation [14] with Langer's modification [15], DCS were calculated by partial wave analysis for varied spatial orientations in the center-of-mass system (CMS), which, in the present case, are characterized by the orientational angle θ.

According to the IOS formula [6]

$$I(\vartheta) = \frac{1}{2}\int_{-1}^{1} I(\theta, \vartheta)\, \mathrm{d}(\cos\theta), \tag{14}$$

where ϑ describes the CMS scattering angle, the DCS were computed applying a 32 point Gauß-Legendre quadrature for averaging with respect to θ.

In order to fit these DCS to the experimental (i. e. laboratory) results, the computed DCS were to be transformed to the laboratory frame using the elastic *Jacobian*. Results of this transformation were then averaged with respect to the velocity and angular distribution of the beams, and to the finite aperture of the detection device [16].

IV. Results and Discussion

A) Anisotropic Interaction Potentials

Experimental DCS's which may be used with other potential models are given in Table 2. Figure 1 presents both, measured and computed DCS for each of the systems under investigation. As can be seen,

*Erratum: In [4] $f(r) = f_{rep}(r) + f_{att}(r)d(r)$ is missed behind equation (3).

Table 2. Experimental total cross section measurements.

	He-C_2H_6		He-1,1-$C_2H_4F_2$		He-1,1,1,2-$C_2H_2F_4$		He-C_2F_6	
Θ	$I(\Theta)$	$\Delta I(\Theta)$	$I(\Theta)$	$\Delta I(\Theta)$	$I(\Theta)$	$\Delta I(\Theta)$	$I(\Theta)$	$\Delta I(\Theta)$
3.0	10000.00	231.35	10000.00	181.92	10000.00	192.66	10000.00	223.29
3.4	8957.52	217.98	6294.06	168.61	7372.69	86.82	7916.07	145.51
3.8	7601.46	115.80	5493.26	108.12	6492.15	81.91	7487.22	64.34
4.2	6105.14	129.09	4984.50	69.91	6347.20	98.58	6975.50	91.58
4.6	4499.59	59.74	4285.07	34.88	5514.26	61.05	6178.57	114.61
5.0	3065.95	39.59	3375.30	63.75	4454.30	61.78	4905.95	74.56
5.4	1854.91	31.01	2191.74	34.26	3069.77	39.12	3448.40	48.36
5.8	1183.47	22.51	1454.92	27.82	1896.27	26.09	2052.73	31.00
6.2	1005.94	18.53	936.73	16.82	1318.92	23.54	1406.61	19.62
6.6	1158.56	11.18	848.90	15.85	1186.40	23.51	1350.17	22.60
7.0	1294.04	15.25	922.39	10.41	1271.65	20.06	1488.35	15.81
7.4	1325.97	17.62	1017.00	13.64	1375.47	13.83	1615.68	17.69
7.8	1186.66	16.48	1023.51	12.18	1376.44	20.79	1634.49	21.03
8.2	961.22	15.14	904.20	8.77	1194.93	12.46	1388.87	17.49
8.6	701.53	12.77	727.13	12.30	923.37	12.80	1039.60	10.42
9.0	480.93	8.31	515.70	8.89	677.63	15.04	713.79	16.25
9.4	324.88	9.13	344.73	6.54	428.51	11.47	450.62	10.07
9.8	284.28	7.39	238.92	10.56	319.61	6.79	349.56	12.85
10.2	308.28	7.28	199.61	7.43	280.68	10.44	332.74	10.42
10.6	346.89	6.75	228.76	5.51	330.81	7.76	422.09	5.20
11.0	375.58	7.09	256.45	6.00	388.57	11.71	463.85	8.97
11.4	366.86	8.39	283.64	6.33	396.30	7.44	484.57	10.00
11.8	336.02	7.43	277.13	4.82	380.08	7.53	442.45	10.71
12.2	275.46	6.15	241.97	2.53	300.98	7.55	354.93	7.61
12.6	239.42	5.93	199.74	4.18	229.55	5.81	271.58	7.60
13.0	195.55	8.27	159.24	5.50	183.76	4.62	194.41	6.05
13.4	181.79	5.87	124.74	5.21	136.74	6.39	158.44	5.67
13.8	161.12	4.68	110.86	7.03	134.82	3.80	153.07	6.22
14.2	164.34	5.50	107.45	4.74	121.44	5.36	155.94	6.23
14.6	149.02	8.16	105.21	4.51	138.62	6.31	173.63	6.97
15.0	155.69	5.04	105.95	3.28	140.92	6.15	171.21	5.46
15.4	150.81	4.96	105.32	2.93	146.49	8.53	168.68	5.53
15.8	140.25	5.77	101.83	4.18	133.89	5.86	139.52	4.41
16.2	140.08	4.13	92.85	3.98	111.82	4.34	132.61	5.10
16.6	109.96	5.56	83.45	6.24	98.23	3.15	109.19	5.82
17.0	121.08	5.30	77.68	3.14	90.94	4.03	101.16	4.09
17.4	109.81	4.46	63.47	2.84	81.79	5.26	106.51	5.81
17.8	115.71	4.44	67.57	3.51	77.39	2.63	93.66	4.30
18.2	106.83	5.80	64.75	3.92	73.00	5.09	92.13	3.75
18.6	103.95	3.97	67.08	2.89	87.45	5.61	81.87	5.45
19.0	107.08	3.72	62.53	3.42	83.66	4.68	93.91	6.85
19.4	95.27	3.82	62.65	2.56	73.45	3.11	82.89	5.54
19.8	92.44	4.77	60.51	3.58	58.54	4.06	78.12	6.18
20.2	80.21	4.38	55.98	3.01	60.60	6.44	74.10	8.15
20.6	84.65	3.30	54.64	2.96	60.78	3.17	64.33	4.12
21.0	84.77	3.10	50.96	2.61	57.68	4.07	68.28	5.14
21.4	81.65	5.26	50.59	3.11	61.32	7.84	63.39	3.35
21.8	75.37	3.75	45.80	2.52	60.65	4.97	59.76	4.40

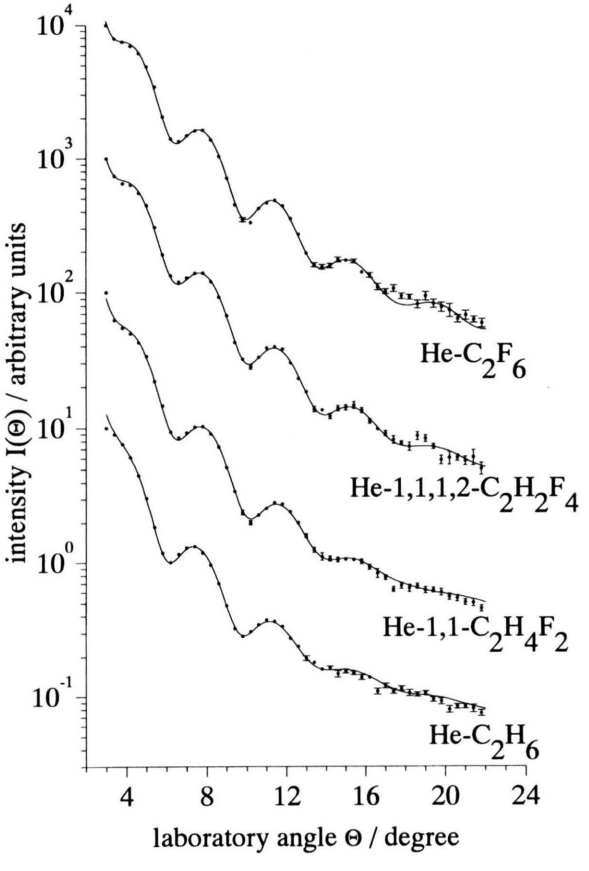

Fig. 1. Laboratory differential cross sections for the scattering of He by $C_2H_xF_{6-x}$ ($x = 0, 2, 4, 6$). The ordinates are shifted arbitrarily. Points with error bars are experimental measurements of the total differential cross section. Solid lines are calculated using best-fit potentials extracted from measured data.

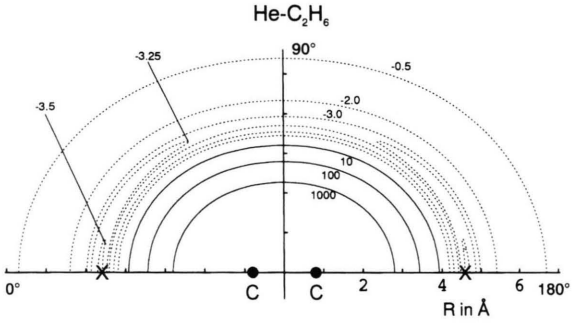

Fig. 2. He-C_2H_6 potential energy surface calculated from the best-fit anisotropic HFD-parametrization. Contours are given in meV. Dotted lines represent the attractive part, solid lines the repulsive part of the potential. Absolute minima are denoted by X.

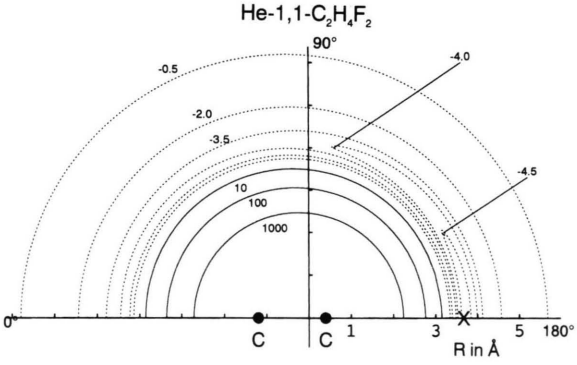

Fig. 3. He-1,1-$C_2H_4F_2$ potential energy surface. Explanations as in Figure 2.

damping of the diffraction oscillations increases slightly with decreasing number of fluorine atoms in the molecules. Parameters for the best-fit potentials are compiled in Table 3. Contour maps of the potential energy surfaces are shown in Figs. 2 to 5.

Table 3. Best-fit potential parameters.

Parameter	He-C_2H_6	He-1,1-$C_2H_4F_2$	He-1,1,1,2-$C_2H_2F_4$	He-C_2F_6
ε_0 [meV]	3.22	4.09	4.55	4.51
ε_1 [meV]	–0.05	–0.10	–0.10	–0.06
ε_3 [meV]	—	–0.40	–0.49	—
ε_4 [meV]	0.33	0.17	0.31	0.95
R_0 [pm]	391	418	438	447
R_1 [pm]	–6	–5	–6	–16
R_2 [pm]	–1.28	–0.85	–0.65	–1.21
R_3 [pm]	—	44	42	—
R_4 [pm]	75	–2	13	65
c_6	0.93	1.18	0.97	0.99
c_8	0.68	0.60	0.67	0.57
c_{10}	0.61	0.37	0.56	0.40
a	1.50	0.99	1.03	0.81
b	13.63	13.14	13.62	14.96

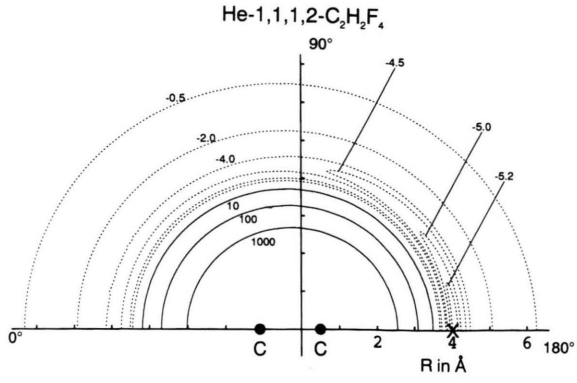

Fig. 4. He-1,1,1,2-$C_2H_2F_4$ potential energy surface. Explanations as in Figure 2.

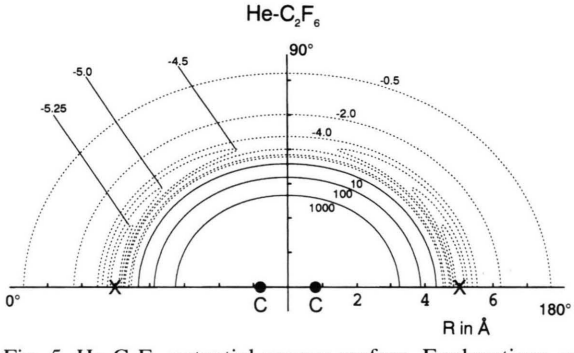

Fig. 5. He-C_2F_6 potential energy surface. Explanations as in Figure 2.

Anisotropy of the well-depth may be recognized for each system. It is found most pronounced for two different collisional orientations:

1) the He atom approaches perpendicular to the C-C axis.

2) the He atom approaches in-line with the C-C axis.

In the latter case two different in-line orientations exist for molecules such as 1,1-Difluoroethane or 1,1,1,2-Tetrafluoroethane. Well-depth minima for these orientations are given in Table 4; corresponding potential curves are shown in Figure 6.

Obviously, for the perpendicular case, the distances R_m of the potential minima for He-Ethane and He-Hexafluoroethane are close to those for the almost spherical systems He-CH_4 (378 pm [2]) and He-CF_4 (396 pm [3]). Expectedly the respective in-line results are found to be larger, the difference corresponding approximately to about one half of a C-C bond length (154 pm [17]). For an in-line approach of the He atom

	He-C_2H_6	He-C_2H_6 [18]	He-1,1-$C_2H_4F_2$	He-1,1,1,2-$C_2H_2F_4$	He-C_2F_6
$R_{m\perp}$ [pm]	376 (375)	381	409 (414)	427 (405)	412 (412)
$R_{m\parallel(0°)}$ [pm]	459 (456)	483	455 (472)	486 (501)	501 (491)
$R_{m\parallel(180°)}$ [pm]	459 (456)	483	367 (457)	392 (464)	501 (491)
$\varepsilon_{m\perp}$ [meV]	3.10 (3.04)	3.74	3.91 (3.50)	4.38 (3.99)	4.37 (4.42)
$\varepsilon_{m\parallel(0°)}$ [meV]	3.50 (3.70)	1.05	3.68 (3.99)	4.27 (4.52)	5.40 (5.19)
$\varepsilon_{m\parallel(180°)}$ [meV]	3.50 (3.70)	1.05	4.64 (6.07)	5.25 (6.68)	5.40 (5.19)

Table 4. R_m and ε_m-values for characteristic orientations (data in brackets are calculated using a different anisotropy model [1] similar to the one used by Keil et al. [18]).

System	He-CF_4 [3]	He-CHF_3 [19]	He-1,1,1,2-$C_2H_2F_4$	He-C_2F_6
ε_m for in-line approach on a F_3C-group	5.33	5.13	5.25	5.4

Table 5. Well depth for a He approach towards a F_3C-group.

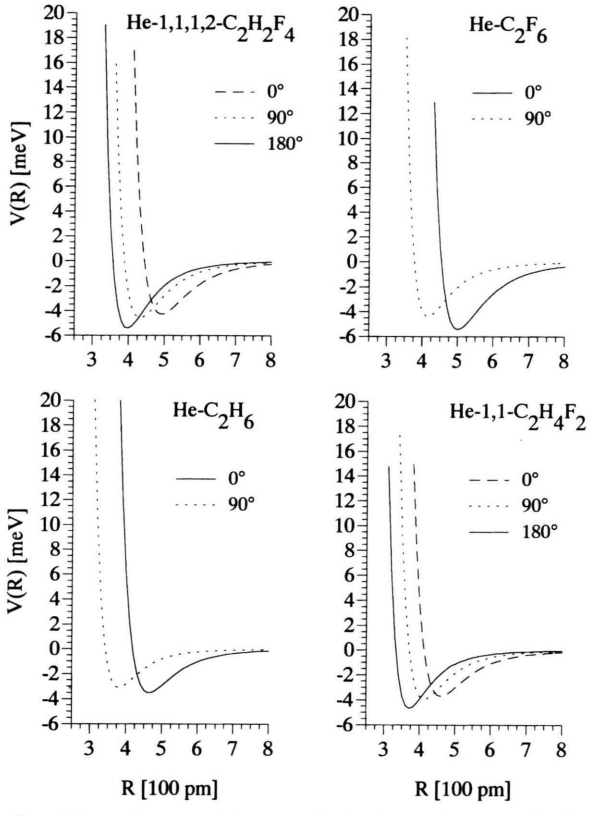

Fig. 6. Best-fit potential curves for in-line and perpendicular approach of the He atoms.

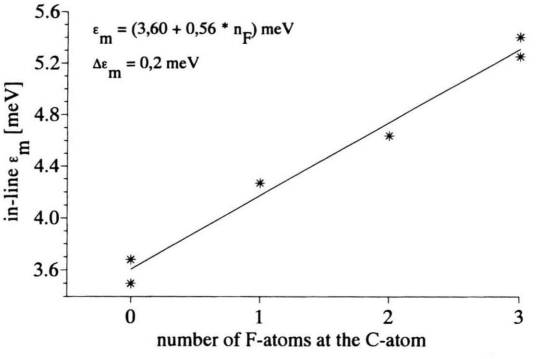

Fig. 7. Well-depth for in-line approach depending on the number of subsituting fluorine atoms.

towards the F_3 plane of 1,1,1,2-Tetrafluoroethane or Hexafluoroethane the well depths are found similar to results for He-F_3CH [19] and He-F_3CF, respectively [3] (Table 5). Comparing results for He approaching in-line to the differently substituted methyle groups of the ethanes the well depths are found to depend linearly on the number of fluorine atoms (Figure 7).

Contrary to the range parameters (R_m) for He-C_2H_6, which agree well with data of Keil et al. [18], the energy parameters ε_m of the present potential are different from the respective results of these authors. In addition the equilibrium configuration He-C_2H_6 is found to be linear (not T-shaped), i. e. the absolute minima of the well-depth exist for either in-line approach of the He atom. This is equivalent to the findings for the Fluoroethanes. Considering the model dependent differences in ε_m, we calculated best fit potential parameters for a potential model which has been used previously [1] and which is quite similar to the one used by Keil et al. [18]. In this case, results for R_m and ε_m correspond to our present results. But ε_m results from this model appear not to be very likely (Table 5) in the case of the fluoroethanes. Thus, from the consistency of the results of Table 5 and from the linearity of the ε_m data (in-line, Fig. 7) we assume our potentials to be reliable. Since from experimental DCS to the "true" interaction potential no direct route is available, several potential models may be used to portray molecular interaction for scattering of atoms by various molecules [7, 20, 21]. Thus, data calculated for the same system usually turn out to be slightly different if suitable potential models are used for which modelling of the molecular anisotropy is somewhat different.

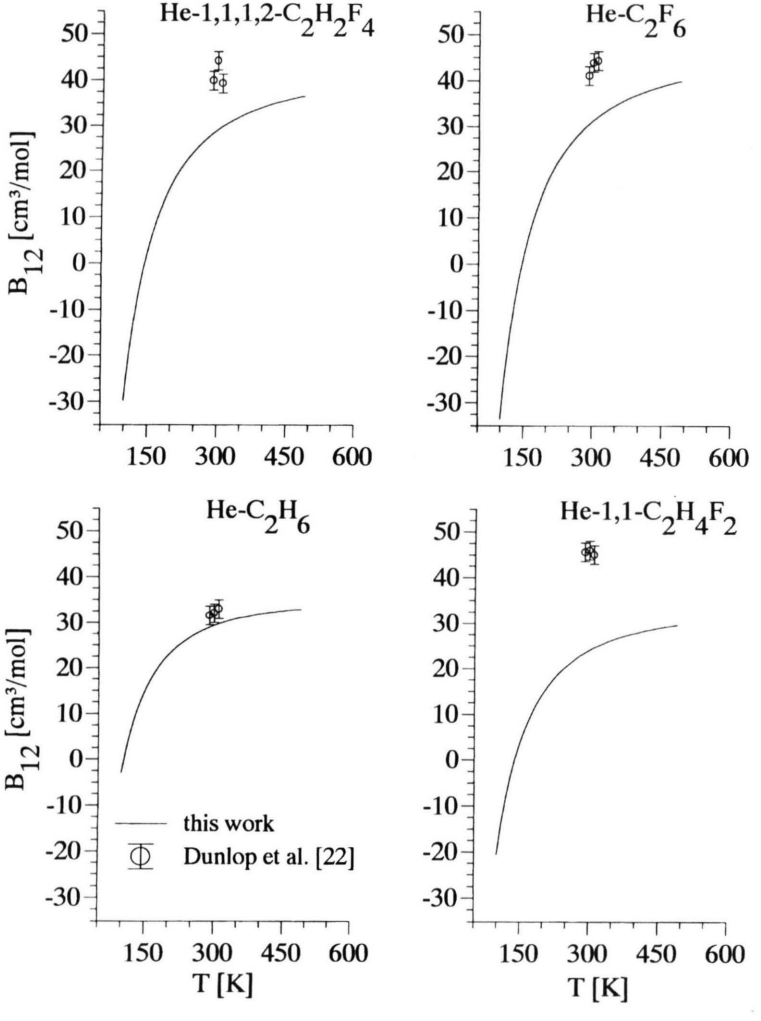

Fig. 8. Calculated second virial coefficients B_{12} as functions of temperature. Points with error bars are experimental data of Dunlop et al. [22].

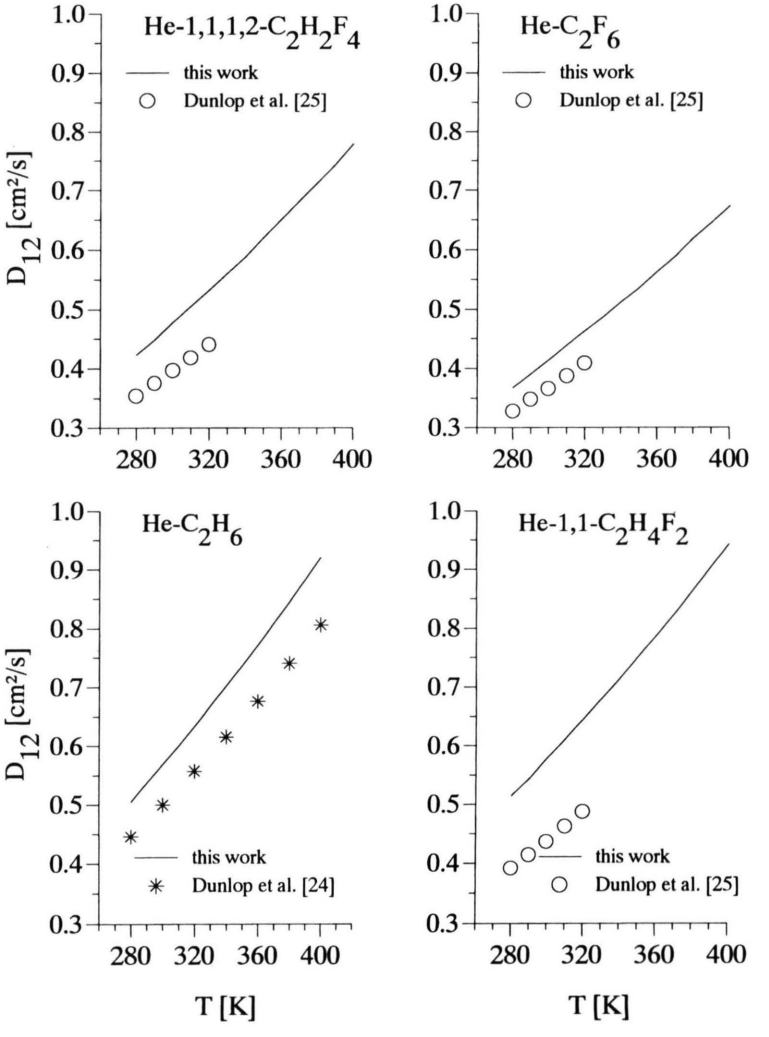

Fig. 9. Diffusion coefficients D_{12} as functions of temperature (p = 1.013 bar). Points are experimental data of Dunlop et al. [24, 25].

B) Macroscopic parameters

Once the interaction potential $V(r, \theta)$ is known, binary macroscopic paramaters such as the second virial coefficient B_{12}, the diffusion coefficient D_{12} and the viscosity coefficient η_{12} may be calculated as described in [3]. Using results from Table 3, heterogeneous second virial coefficients were computed for the temperature range 100 K < T < 500 K (Figure 8). For comparison, values for 290 K, 300 K, and 310 K are available from macroscopic investigations of Dunlop et al. [22].

Binary diffusion coefficients and the coefficients of viscosity were computed via respective collision integrals [23]. D_{12} data are given for 280 K < T < 400 K in Figure 9 together with results of Dunlop et al. [24, 25]. Deviations range between 12 % and 25 %. As has been shown by Maitland [26] for the system He-CO_2 such deviations may be due to the Mason and Monchick approximation [27] which was used in our calculations.

Coefficients of viscosity were computed for 1.013 bar and 298 K to a first order approximation according to [23]. Results are presented in Figure 10. Viscosities

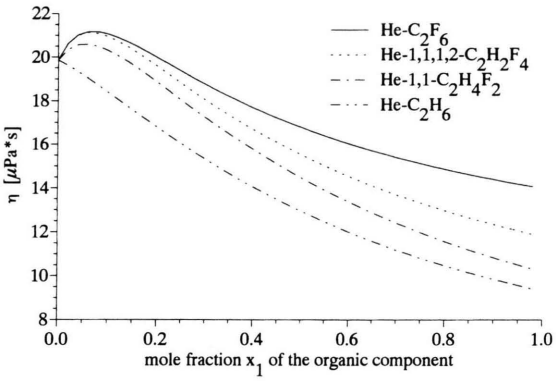

Fig. 10. Viscosities for T = 298 K and p = 1.013 bar.

for the pure substances were used as He: 19.86 μPa·s; C_2H_6: 9.3 μPa·s, 1,1-$C_2H_4F_2$: 10.2 μPa·s, 1,1,1,2-$C_2H_2F_4$: 11.8 μPa·s and C_2F_6: 14.0 μPa·s [28].

Acknowledgement

Support by the Fonds der Chemischen Industrie, the Hoechst AG, Werk Cassella and the Deutsche Forschungsgemeinschaft is gratefully acknowledged.

[1] R. Brandt, M. Henkel, B. Pfeil, and W. Seidel, J. Chem. Phys. **95**, 135 (1991).
[2] M. Henkel, B. Pfeil, and W. Seidel, J. Chem. Phys. **96**, 5054 (1992).
[3] C. Gebauer, O. Klein, R. Schmidt, and W. Seidel, Z. Naturforsch. **50a**, 468 (1995).
[4] R. Schmidt, C. Gebauer, O. Klein, and W. Seidel, Z. Naturforsch. **52a**, 317 (1997).
[5] C. Gebauer, O. Klein, R. Schmidt, and W. Seidel, Z. Naturforsch. **52a**, 425 (1997).
[6] G. A. Parker, and R. T. Pack, J. Chem. Phys. **68**, 1585 (1978) and references therein..
[7] U. Buck, V. Khure, and M. Kick, Mol. Phys. **35**, 65 (1978).
[8] R .T. Pack, Chem. Phys. Lett. **55**, 197 (1979).
[9] G. Rotzoll, and A. Lübbert, J. Chem. Phys. **71**, 2275 (1979).
[10] R. A. Aziz, P. W. Riley, U. Buck, G. Maneke, J. Schleusener, G. Scoles, and U. Valbusa, J. Chem. Phys. **71**, 2637 (1979).
[11] C. Douketis, G. Scoles, S. Marchetti, M. Zen, and A. J. Thakkar, J. Chem. Phys. **76**, 3057 (1982).
[12] O. E. Klein, Private communication.
[13] J. Frick, Bericht 9, Max-Planck-Institut für Strömungsforschung Göttingen(1984).
[14] M. S. Child, Molecular Collision Theory, Academic Press, London and New York (1974).
[15] R. E. Langer, Phys. Rev. **51**, 669 (1937).
[16] M. Henkel, Dissertation, Justus-Liebig-Universität Gießen 1991.
[17] L. S. Bartell and H. K. Higginbotham, J. Chem. Phys. **42**, 851 (1965).
[18] L. J. Danielson, M. Keil, and P. J. Dunlop, J. Chem. Phys. **88**, 4218 (1988).
[19] M. Hammer, Dissertation, Justus-Liebig-Universität Giessen 1997.
[20] U. Buck, J. Schleusener, and F. Huisken, J. Chem. Phys. **89**, 2886 (1988).
[21] L. Beneveti, P. Casavecchia, F. Vecchiocattivi, G. G. Volpi, U. Buck, Ch. Lauenstein, and R. Schinke, J. Chem. Phys. **89**, 4671 (1988).
[22] C. M. Bignell and P. J. Dunlop, J. Chem. Phys. **98**, 4889 (1993).
[23] J. O. Hirschfelder, C. F. Curtiss, and R. B. Bird, Molecular Theory of Gases and Liquids, John Wiley and Sons, New York 1964.
[24] P. J. Dunlop and C. M. Bignell, J. Chem. Phys. **93**, 2701 (1990).
[25] P. J. Dunlop and C. M. Bignell, J. Chem. Phys. **97**, 5638 (1992).
[26] G. C. Maitland, V. Vesovic, and W. A. Wakeham, Mol. Phys. **42**, 803 (1981).
[27] L. Monchick and E. A. Mason, J. Chem. Phys. **35**, 1676 (1961).
[28] Beilstein, STN-Database, Karlsruhe 1996.